SCIENCE CHINA
Information Sciences

July 2020, Vol. 63 170107:1–170107:3
https://doi.org/10.1007/s11432-019-2819-y

• LETTER •
Special Focus on Brain Imaging and Addiction

Dysfunctional resting-state EEG microstate correlated with the severity of cigarette exposure in nicotine addiction

Yan CHENG[1†], Junjie BU[2*†], Nan LI[3], Jian LI[4], Huixing GOU[4], Shinan SUN[5], Chang LIU[4], Zida JIN[4], Changle HE[2], Chuan FAN[6], Chialun LIU[4] & Xiaochu ZHANG[1,4,5*]

[1]*School of Humanities and Social Science, University of Science and Technology of China, Hefei* 230026*, China;*
[2]*School of Biomedical Engineering, Research and Engineering Center of Biomedical Materials, Anhui Medical University, Hefei* 230032*, China;*
[3]*Lab for Cognitive Brain Mapping, RIKEN Center for Brain Science, Wako* 3510198*, Japan;*
[4]*Eye Center, Department of Ophthalmology, the First Affiliated Hospital of USTC, Hefei National Laboratory for Physical Sciences at the Microscale, School of Life Sciences, Division of Life Sciences and Medicine, University of Science and Technology of China, Hefei* 230027*, China;*
[5]*Academy of Psychology and Behavior, Tianjin Normal University, Tianjin* 300387*, China;*
[6]*Department of Medical Psychology, the First Affiliated Hospital of Anhui Medical University, Hefei* 230022*, China*

Received 29 November 2019/Revised 4 February 2020/Accepted 11 March 2020/Published online 1 June 2020

Citation Cheng Y, Bu J J, Li N, et al. Dysfunctional resting-state EEG microstate correlated with the severity of cigarette exposure in nicotine addiction. Sci China Inf Sci, 2020, 63(7): 170107, https://doi.org/10.1007/s11432-019-2819-y

Dear editor,

Nicotine is a significant cause of severe physical and psychiatric disorders. Evidence suggests that smokers have poorer global cognitive functioning in later life, as well as lower average scores in several cognitive domains, including cognitive flexibility and memory [1]. There are large numbers of electroencephalography (EEG) such as event-related potential, the late positive potential, the low-theta EEG coherence network studies in nicotine addiction. These traditional EEG methods provided a rich insight into the electrophysiology with a high temporal resolution, however, they did not reflect the transient stable and global functional pattern of the brain. Microstate analysis is an alternative approach based on global topography analysis. EEG microstate as a tool is widely used in neuropsychiatric disease, but this approach has rarely been used in addiction research.

Microstate is defined by the topography of electric potentials recorded in a multi-channel electrode cap, which remains stable for 60–120 ms before rapidly transiting to a different microstate [2]. The microstate with its associated spatial topography may reappear in time, and is referred to microstate class. Microstate duration represents the same microstate labels allocated during all successive maps. Additionally, microstate occurrence represents the mean number of occurrences of each microstate class per second and microstate coverage calculated by the percentage of total duration covered by each microstate class within the overall analysis period. Microstate has rich syntactic structures that include a vast amount of important information about the cognitive process.

Our study attempts to explore the relationship between indicators of resting-state EEG microstate and the severity of cigarette exposure and the degree of nicotine dependence. In our current study, with microstate analysis, we find that microstate class B and D topographies are significantly different in the smoking group compared to

* Corresponding author (email: bujunjie@ahmu.edu.cn, zxcustc@ustc.edu.cn)
† Yan CHENG and Junjie BU have the same contribution to this work.

the control group. In microstate temporal characteristics, we find that the duration, occurrence, and coverage of microstate B in the smoking group are significantly different from those in the control group. Moreover, the microstate B duration is negatively correlated with the severity of tobacco consumption.

Participants. Twenty smokers are involved in this experiment who meet the criteria in our previous study [3]. Twenty-one control participants with no smoking history, matched with age [mean = 21.8 and SD = 1.8], gender, and education years [mean = 15.3 and SD = 1.1] are recruited. All participants are recruited by Internet advertisements and posters. Demographic and clinical characteristics are available in Appendix A.1. All participants signed written informed consent before the study. The degree of nicotine dependence is measured by Fagerstrom Test of Nicotine Dependence (FTND) [4], and pack-years is used to test the degree of exposure to nicotine. And the inclusion criteria and exclusion criteria see Appendix A.2.

EEG recording and preprocessing. Resting-state EEG data is acquired using a Neuroscan SynAmps RT amplifier comprising 64 Ag/AgCl electrodes placed on the participant's scalp following the position of the extended international 10-20 system. The impedance of all electrodes is kept below 5 kΩ. Data are collected of continuous 5 min at a sampling rate of 500 Hz. The preprocessing procedure is performed in MATLAB EEGLAB toolbox (MathWorks, R2019a). Data preprocessing followed basic principles in previous literature [5]. Briefly, for spontaneous continuous EEG data, first, artifact should be removed and corrected for cleaning the EEG data. Second, the EEG data should be recomputed against the average reference. Third, the EEG data should be filtered (e.g., 1–30 Hz). EEG segments with eye movements, electromyograms, and other significant artifacts are removed. Data are then downsampled at 250 Hz, bandpass filtered between 2–20 Hz and re-reference to the average reference.

EEG microstate analysis. The microstate analysis consists of the following procedures [2, 5, 6]. First, global field power (GFP) is extracted which represents global brain activity. The formula is as follows:

$$\mathrm{GFP}(t) = \sqrt{\frac{\sum_i^N (V_i(t) - \overline{V}(t))^2}{N}}, \qquad (1)$$

where $V_i(t)$ represents the electric potential of the ith electrode (i = 1:60 electrodes) at time t, N represents the number of electrodes, $\overline{V}(t)$ represents the mean of instantaneous potentials across all electrodes, and the GFP(t) means the spatial standard deviation of the EEG signal across all electrodes. The local maxima of GFP represent the instants of the strongest field strength and the highest signal-to-noise ratio [7]. EEG topographies tend to be stable around the peaks of GFP and change rapidly near the local minima of GFP. Thus, the EEG signal map at each GFP peaks is selected for segmentation.

Second, for each participant, topographies at GFP peaks are subjected to a k-means clustering, which is a well-established clustering method. At first, in individual level, we have tested the range of 3 to 8 classes for each participant individually. Global explained variance (GEV) is used to setting the number of microstate clusters. According to GEV criteria (Appendix A.3.1), the number of microstate classes is set to four for all subsequent analyses. In each subject, all possible permutations of the 4 individual microstate maps were best fitted with the 4 prototype maps. The prototypes were updated by averaging the best-fit permutated individual microstate maps. The 4 classes are then averaged across all participants within each group using a permutation algorithm that maximizes the common variance over subjects [8] and overall maps across all participants are calculated by averaging the group-level maps from the two groups.

Third, the overall mean maps for all microstate classes are then fit back to the original data at GFP peaks. We assign each GFP peak to one of the microstate classes based on the maximal spatial correlation between topographies [6]. Microstate class labels are interpolated between halfway of two GFP peaks (Appendix A.3). The mean global explained variance of the smoking group and the control group are 77.16% (SD = 6.8%) and 75.3% (SD = 5.7%), respectively. Finally, microstate duration, microstate occurrence and microstate coverage are calculated. Microstate statistics see Appendix B.1 for a more detailed description.

Microstate topographies. The smoking group, the control group and the overall group maps of all the participants are shown in Figure 1(a). The overall TANOVA reveals a main effect of group between the smoking group and the control group (p <0.001) and a main effect of the four microstate classes (p = 0.002), but no interaction between the group and class factors (p = 0.155). However, post hoc analysis shows that the microstate topographic maps of the smoking group and the control group are significantly different in class B and D, while there are no significant differences in microstate class A and C.

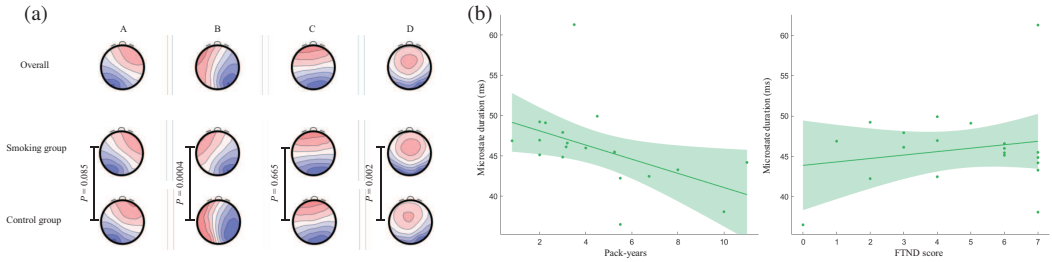

Figure 1 (Color online) Microstate topographies (a) and correlations between behavior and microstate duration (b).

Microstate parameters characteristics. We find that the duration of microstate B is shorter in the smoking group (46 ms) compared with the control group (51 ms) ($t(39) = -3.1$, $p = 0.004$, subfigure A in Figure S2). The occurrence of microstate B significantly is lower in the smoking group (3.53 per second) compared with the control group (4.36 per second) ($t(39) = -2.524$, $p = 0.016$, subfigure C in Figure S2). Accordingly, the coverage of microstate B in the smoking group (0.16) is significantly less than the control group (0.22) ($t(39) = -3.61$, $p < 0.001$, subfigure C in Figure S2). There are no significant group differences in the duration, occurrence and coverage of the microstate classes of A, C and D shown in Appendix B.3.

Correlations between behavior and microstate. No significant correlation is observed between pack-years and FTND score in the smoking group ($r(39) = 0.383$, $p = 0.096$). Figure 1(b) shows a significant correlation is found between pack-years and the duration of microstate B in the smoking group ($r(39) = 0.480$, $p = 0.032$) and there is no significant correlation between FTND score and the duration of microstate B in the smoking group ($r(39) = 0.414$, $p = 0.193$).

Conclusion. There were three major findings in this study. First, in the topography structure of the two groups, we found a significant difference in microstate maps B and D. Second, in the specific microstate B, we found that the duration of microstate in the smoking group was significantly shorter than that in the control group. Finally, in the smoking group, we found that the duration of microstate B was negatively correlated with pack-years, while there was no correlation between the duration of microstate B and FTND score. Collectively, this study is the first one to apply the resting-state EEG microstate approach to investigate nicotine addiction. Moreover, our results suggest that the duration of microstate class B is a novel objective biomarker for monitoring the severity of cigarette consumption in smokers.

Declaration The research protocol was approved by the Human Ethics Committee of the University of Science and Technology of China.

Acknowledgements This work was supported by National Key Basic Research Program (Grant Nos. 2016YFA0400900, 2018YFC0831101), National Natural Science Foundation of China (Grant Nos. 71942003, 31771221, 61773360, 71874170), School Foundation of Anhui Medical University (Grant No. 2019xkj016, XJ201907), National Science Foundation for Young Scientists of China (Grant No. 31900766), Major Project of Philosophy and Social Science Research, Ministry of Education of China (Grant No. 19JZD010), Fundamental Research Funds for the Central Universities of China.

Supporting information Appendixes A and B. The supporting information is available online at info.scichina.com and link.springer.com. The supporting materials are published as submitted, without typesetting or editing. The responsibility for scientific accuracy and content remains entirely with the authors.

References

1 Corley J, Gow A J, Starr J M, et al. Smoking, childhood IQ, and cognitive function in old age. J Psychosomatic Res, 2012, 73: 132–138
2 Khanna A, Pascual-Leone A, Michel C M, et al. Microstates in resting-state EEG: current status and future directions. Neurosci Biobehaval Rev, 2015, 49: 105–113
3 Bu J, Ma R, Fan C, et al. Low-Theta electroencephalography coherence predicts cigarette craving in nicotine addiction. Front Psychiatry, 2019, 10: 296
4 Heatherton T F, Kozlowski L T, Frecker R C, et al. The fagerstrom test for nicotine dependence—a revision of the fagerstrom tolerance questionnaire. Brit J Addict, 1991, 86: 1119–1127
5 Michel C M, Koenig T. EEG microstates as a tool for studying the temporal dynamics of whole-brain neuronal networks: a review. Neuroimage, 2018, 180: 577–593
6 Schumacher J, Peraza L R, Firbank M, et al. Dysfunctional brain dynamics and their origin in Lewy body dementia. Brain, 2019, 142: 1767–1782
7 Lehmann D, Skrandies W. Reference-free identification of components of checkerboard-evoked multichannel potential fields. Electroencephalography Clin Neurophysiol, 1980, 48: 609–621
8 Koenig T, Lehmann D, Merlo M C G, et al. A deviant EEG brain microstate in acute, neuroleptic-naive schizophrenics at rest. Eur Archives Psychiatry Clin Neurosci, 1999, 249: 205–211